GPGPU Monte Carlo Calculation of Gyro-Phase Resolved Fast Ion and n-State Resolved Neutral Deuterium Distributions

R.J.Akers[1], E.Verwichte[2], T.J.Martin[1], S.D.Pinches[1], R.Lake[1,2]

[1]EURATOM/CCFE Fusion Association, Culham Science Centre, Abingdon, Oxon OX14 3DB, UK.
[2]Centre for Fusion, Space and Astrophysics, Department of Physics, University of Warwick, Coventry CV4 7AL, UK.

Abstract

In order to calculate the fast particle instability drive in a neutral beam or ICRH heated tokamak plasma, it is necessary to construct a fast ion distribution function F that is both a) high resolution and b) smooth, as drive and damping terms depend upon gradients in real and velocity space. We describe briefly here, a new Monte Carlo algorithm (**LOCUST-GPU**), designed to calculate the full gyro-orbit (rather than guiding centre), high resolution, fast ion distribution without the need for any post-process smoothing. The code uses the latest generation of GPGPU co-processor hardware, with the tracking algorithm cast across multiple GPUs using OpenMP threads, deployed as a PGI-FORTRAN CUDA kernel on each GPU device (with sum reduction of the GPU threads taking place on the CPU host). For toroidally symmetric plasma, a goosing algorithm similar to that used by TRANSP/NUBEAM can be applied, allowing ~10^7 ions to be tracked to thermalization in ~10 hours using 4 no. GTX580 cards, with a typical error per cell of order ~1% (using 340 P_ϕ cells, 125 μ cells and 120 velocity/energy cells). We also report on the development of a GPU based bundled-n collisional radiative solver (required for tracking beam-neutrals and hydrogenic neutrals resulting from charge exchange).

1. Orbit tracking

Charged particles are tracked by solving the Lorentz equations of motion, either in cylindrical or Cartesian coordinates (depending upon the integrator being deployed – 6 are available). The two most notable are the error controlled Runge-Kutta RK45 (Cash-Karp [1]) and the widely used Boris leap-frog scheme [2]. The former is slow but with controllable accuracy (and therefore useful for testing), the latter is fast and adequate for a wide range of physics (having been extensively benchmarked here against RK45). In order to couple LOCUST-GPU to codes such as HAGIS [3], various options are available for storing or passing F. Real space coordinates can be used (in 5D, i.e. gyro-phase resolved if necessary), or a more compact constants of motion (COM) space representation $\{E,P_\phi,\mu,\sigma\}$. Here, E is the particle energy, P_ϕ the canonical angular momentum, μ the magnetic moment (expanded to first order), and σ the sign of the instantaneous guiding centre pitch λ ($=V_{||\_GC}/V$) (to first order). First order expansion of μ is necessary for reducing oscillations present in μ_0 in low field devices such as MAST and NSTX, and for reducing smearing of the Monte Carlo generated Jacobian $\mathfrak{J}$ and F. Separation in σ is required in order to discriminate the majority of trapped and passing orbits (only a small fraction of type III and type IV orbits [4] remain degenerate). To determine P_ϕ, it is necessary to accurately and simultaneously determine velocity and spatial location – this is problematic for the Boris scheme, where space and velocity increments are separated by half a time step, resulting in gyro-oscillations. We ameliorate this by dividing the fields by $1-(\Omega_n\Delta t)^2/12$ (the factor by which the zeroth order scheme underestimates gyro-frequency), thereby recovering the efficiency of the

Boris integrator due to its ability to sustain a large time-step. We find that for MAST NBI, a single precision compilation results in a factor ~20 speed-up over double precision RK45, with an acceptable error of 0.006% in E and 0.02% in P_ϕ .

2. Collisions

Collisions are applied using operators based upon the Binomial distribution [5], cast using the formulism from [6]. The error and Chandrasekhar functions can be truncated to zeroth order (for testing against analytic solutions of the Fokker Planck equation), to first order for accurate production runs, or can be included in full for simulating the evolution of thermal ion populations. The code has been extensively tested in both thermal and fast ion regimes against analytic theory.

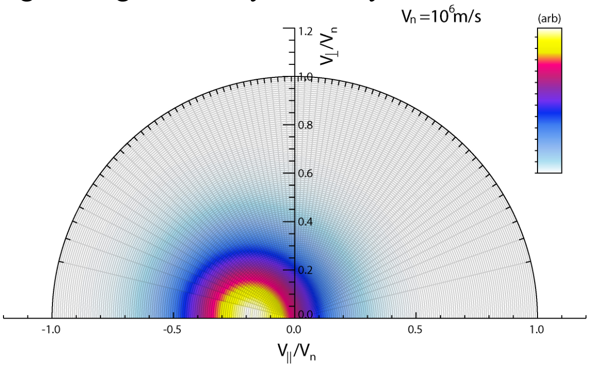

Fig.1: Steady state velocity space distribution resulting from a arbitrary 1eV monotonic source launched in a 1.1keV rotating background plasma.

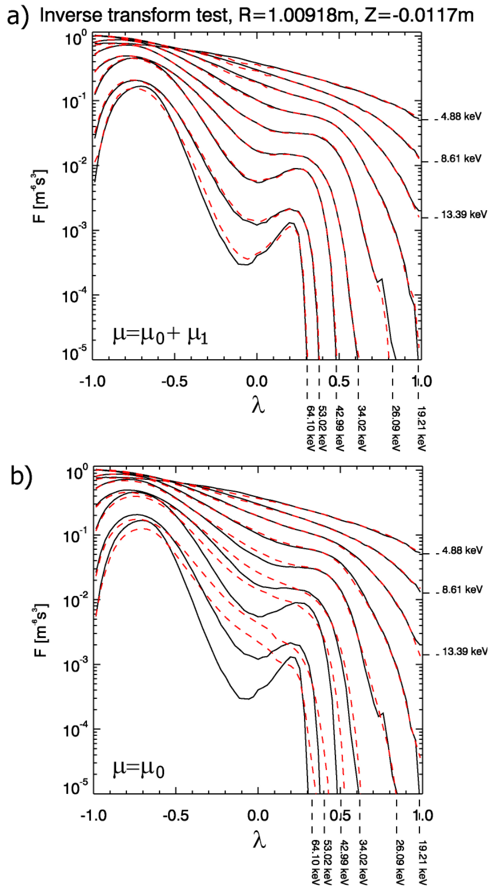

Fig.2: F vs. λ a) using $\mu=\mu_0$ and b) using $\mu=\mu_0+\mu_1$.

Fig. 1. shows the steady state solution in velocity space ($V_\perp/V_n$ vs. $V_{||}/V_n$ where the normalizing velocity V_n=10^{6}m/s) for a 1eV monotonic source launched into a background plasma of 1.1 keV, rotating at 220 krad/s. The Monte Carlo result matches the analytic solution of a boosted 1.1 keV Maxwellian plasma within M.C. stats. Similarly, Monte Carlo calculation of the steady state solution for an energetic 65keV deuterium source, launched as a narrow Gaussian source in λ is in excellent agreement with the analytic solution resulting from expressing the source as a series of Legendre polynomials. Another important test is to quantify the efficacy of storing F in COM space – deployment within codes such as HAGIS inevitably requires a transformation back into real space for generating synthetic diagnostic data. Fig. 2. shows $F(\lambda)$ for various energies at a point within the MAST plasma core. Solid black lines were generated by binning directly in real-space, dotted red lines are for a distribution binned in COM space, then converted back to real space via a GPU based Monte Carlo sampling kernel. a) is the more accurate result with μ_1 correction and b) is the result if μ is truncated to zeroth order (highlighting the error introduced by μ_0 oscillation). Interestingly, the use of COM coordinates introduces a useful level of smoothing via effective "orbit averaging".

3. Typical results

Fig. 3. shows typical results of the Monte Carlo generated real-space to COM space $\mathfrak{I}$ (in the co-direction, σ=+1, for E=63keV) (a & b) as well as F (c & d) against P_ϕ and Λ/B_0 (=μ/E), which for MAST-NBI is heavily biased towards the co-passing region of velocity space. a) and c) are with μ_1 correction, and b) and d) are without – for the latter, F as well as $\mathfrak{I}$ is significantly smeared in the μ direction. Most notably, μ_1 correction sharpens the “real orbit” boundary. Also of note is that the MAST distribution function lies away from the region of degenerate type III and type IV orbits.

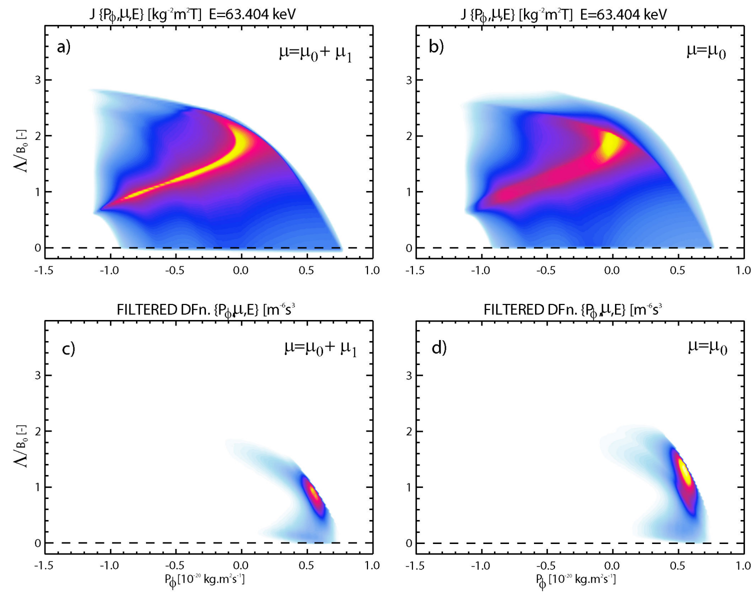

Fig. 3: Real to COM space Jacobian $\mathfrak{I}$ vs. P_ϕ and ΛB_0 (=μ/E) (a & b) and typical MAST NBI distribution function F at 63KeV (c & d). a) and c) include 1st order correction of the magnetic moment.

4. Solution of the Collisional Radiative (C.R.) Equation

In order to develop a next generation NBI code similar to NUBEAM, it is also important to be able to track neutral hydrogenic atoms (in order to provide fast ion sources, account for charge exchange driven redistribution and loss, and for generating synthetic diagnostic data (beam emission (BE), FIDA) etc.). To this end, a C.R. solver has been constructed to complement the LOCUST-GPU charged particle tracker. Cross section data for all the important processes (charge exchange, ionization, collisional excitation/de-excitation and spontaneous emission) are first generated by a pre-processor using the same data as the FIDASim code [7]. The GPU kernel then tracks neutrals through the plasma, solving the C.R. equation for the n-state vector of each neutral. An equilibrium l-state population is assumed throughout. At each time-step, a local C.R. matrix is constructed for each neutral in the Monte Carlo ensemble, by integrating over velocity for the thermal background in the rotating frame of the plasma, and over 3D velocity space for the fast ion population. The code makes no distinction between direct (beam), halo or FIDA neutrals. At each step, a Monte Carlo technique is used to spawn particles for the next generation resulting from charge exchange. Statistics for neutrals born in the n=3 state can be artificially increased, as can statistics for FIDA relative to halo neutrals if the FIDA signal is of more interest. The algorithm can be deployed in low density plasma scenarios (where the fast ion population can be significant), albeit at the expense of a significant CPU overhead (dominated by the integral over F). Fig. 4a) shows the D_α emissivity (log-scale) in the plasma mid-plane, comprising BE, halo and FIDA neutrals. The emission is shifted anti-clockwise around the machine due to toroidal rotation and average drift of the fast ions resulting from co-tangential injection. Fig. 4b) shows a typical D_α spectrum comprising BE, HALO and FIDA emission.

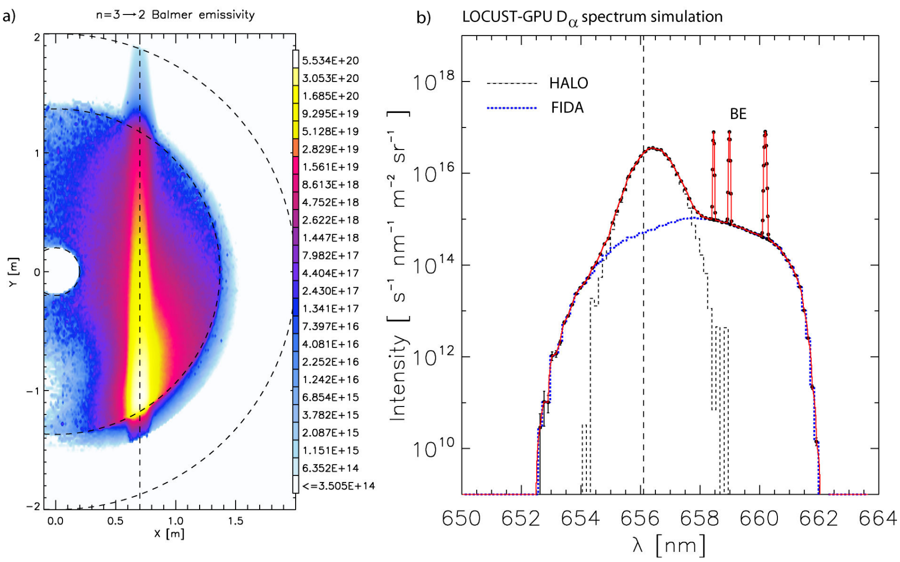

Fig.4: a) LOCUST-GPU mid-plane D_α emissivity and b) a typical synthetic FIDA spectrum (both log-scale).

5. Conclusions

GPU based kernels have been developed for simulating the collisional evolution of charged and neutral hydrogenic ions in tokamak plasmas (including low field devices). Smooth, accurate, high resolution distributions of ions and D_α emission can now be generated in a matter of hours using <£5K of Commercial Off The Shelf desktop hardware eliminating the need for expensive HPC or cluster access. Together, charged and neutral tracking kernels provide a powerful platform for simulating NBI in next generation transport codes, and for detailed MHD analysis. Future work will concentrate on benchmarking against TRANSP and ASCOT, followed by detailed analysis of data from the new MAST FIDA and neutron collimator systems.

References

[1] J. R. Cash & A. H. Karp, 'A variable order Runge-Kutta method for initial value problems with rapidly varying right-hand sides', ACM Transactions on Mathematical Software, Vol.16, No.3, September 1990, p201-222, doi:10.1145/79505.79507.
[2] Boris, J.P. (November 1970). "Relativistic plasma simulation-optimization of a hybrid code". *Proceedings of the* 4th Conference on Numerical Simulation of Plasmas. Naval Res. Lab., Washington, D.C.. pp. 3–67.
[3] S.D.Pinches, L.C.Appel *et al.*, Comput. Phys. Commun. 111 131 (1998).
[4] D.Borba, W.Kerner, J. Comp. Phys. 153, 101-138 (1999).
[5] A.H.Boozer, G.KuoPetravic, Phys. Fluid 24, 851 (1981).
[6] F.Hinton, Handbook of Plasma Physics, Eds. M.N. Rosenbluth & R.Z.Sagdeev, Vol. 1 (1983).
[7] W.W.Heidbrink et al., Commun. Comput. Phys. 10 (2011) 716.

This work was funded by the RCUK Energy programme and EURATOM.